



ELSEVIER

Thermochimica Acta 285 (1996) 11–23

thermochimica
acta

A new flow calorimeter designed for operation to 450°C and 50 MPa

Xuemin Chen, John L. Oscarson, Hongjie Cao¹, Sue E. Gillespie,
Reed M. Izatt*

*Departments of Chemistry and Biochemistry and of Chemical Engineering, Brigham Young University,
Provo, Utah 84602, USA*

Received 2 November 1995; accepted 28 January 1996

Abstract

A new isothermal flow calorimeter for measuring heats of mixing of two fluids at high temperatures is described. The primary use of the calorimeter is for the study of reactions in high-temperature aqueous solutions. The calorimeter was designed for operation to 450°C and 50 MPa for both exothermic and endothermic processes. Platinum–rhodium alloy tubing was used in the calorimeter to resist corrosion by electrolyte solutions under extreme experimental conditions. Preheating of the solutions was achieved by submerging coils of the tubing in a salt bath. An automatically controlled pulsed heater and a constant heat-leak path were used to maintain the reaction zone at a constant temperature. An all-liquid pressure control system was added for operations at higher pressures. Energy effects from 0.0025 to 2 J s⁻¹ can be measured to a precision of ± 1.5% or ± 0.0005 J s⁻¹, whichever is greater. The calorimeter was tested by measuring heats of dilution of aqueous solutions of NaOH at 300°C (9.3 MPa) and of NaCl at 300°C (9.3 MPa) and 350°C (17.6 MPa).

Keywords: Aqueous solution; Flow calorimeter; Heat of mixing; High pressure; High temperature

1. Introduction

Isothermal flow calorimetry is based on measuring the power required to maintain the reaction zone at a constant temperature during the course of a reaction. The

* Corresponding author. Tel.: (801) 378-2315; Fax: (801) 378-5474; E-mail: Reed_Izatt@byu.edu.

¹ Present address: Nu Skin International, Inc., 370 East 1130 South, Provo, Utah 84606, USA.

isothermal condition is achieved in the calorimeter described here by adjusting the power output of a controlled heater to balance the rate of energy production arising from the chemical reaction plus the power removed by a constant heat-leak path. The method is equally applicable to both exothermic and endothermic processes.

A versatile calorimeter is desired for the determination of thermodynamic data for a wide variety of chemical reactions at high temperatures and pressures. High-temperature thermodynamic data are important in many scientific and industrial applications including geochemistry, environmental chemistry, chemical oceanography, hydrometallurgy, electric power plant operation, water desalination, gas processing, and the oxidation of chemical wastes in supercritical water.

Over the last two decades, several versions of isothermal flow calorimeters constructed in our laboratory have been reported [1–7]. We have operated flow calorimeters constructed of stainless steel, Hastelloy-C, tantalum, nickel, platinum–iridium, and platinum–rhodium tubing. The availability of these calorimeters has allowed us to study a variety of systems in the temperature range 15–350°C and pressure range 0.1–17.5 MPa. We have reported the use of isothermal flow calorimetry at high temperatures and pressures for the determination of thermodynamic data for ligand interaction with protons and metal ions in aqueous solutions [8–14], heats of mixing in binary and ternary systems involving organic compounds and carbon dioxide [15–20], and vapor–liquid equilibrium data [21, 22].

This paper describes a new isothermal flow calorimeter for measuring heats of mixing of two fluids (liquid, gas, or supercritical fluid) at high temperatures and pressures. This calorimeter retains all the desirable operating characteristics and advantages of the previous calorimeter [5] while offering additional improvements. By using platinum–rhodium instead of nickel tubing, the new calorimeter has a much improved resistance to corrosion and is capable of operating at high temperatures and high pressures for electrolyte solutions ranging from strongly acidic, to neutral, to strongly basic. Better preheating of the solutions was achieved by submerging the entering coils of the tubing in a salt bath. A new all-liquid pressure control system was added which uses a high-pressure pump running in reverse. The calorimeter was tested by measuring heats of dilution of aqueous solutions of NaOH at 300°C (9.3 MPa) and of NaCl at 300°C (9.3 MPa) and 350°C (17.6 MPa).

2. Description of calorimeter

The present calorimeter is similar to the isothermal high-temperature flow calorimeter for basic solutions described by us [5]. The discussion here will focus primarily on those components that have been changed extensively. The main changes are the use of platinum–10% rhodium tubing in order to resist corrosion by acidic and basic solutions, the use of a salt bath for better preheating to reduce the time required to achieve thermal equilibration, and the addition of an all-liquid pressure control system for operation at higher pressures.

The main components of the new flow calorimeter are the reaction vessel, the isothermal cylinder, the thermal shields and insulating container, the fluid delivery

system containing two high-pressure pumps (Isco 260D) and two pushers, the pressure control system containing a waste solution reservoir and a high-pressure pump running in reverse, the temperature control system that contains four Tronac PTC-41 temperature controllers and a Hart Scientific 3704 isothermal control unit, and the data acquisition system that contains an IBM-compatible (Precision 386SX) computer and an interface (Intelligent DVM by DeltaQuest) between the isothermal control unit and the computer. The pumps are rated for operation at pressures from 0.1 to 51.7 MPa and are equipped with programmable controllers. A schematic diagram of the main components of the calorimeter is given in Fig 1. The reaction vessel and its contents are shown in Fig. 2.

A reaction is initiated by starting the pumps thus expelling the reactants at a constant flow rate from the pushers through the platinum–rhodium tubing so that the two solutions mix in the equilibration coil on the isothermal cylinder (Fig. 2). A controlled heat-leak path removes energy from the isothermal cylinder at a constant rate and discharges it to the reaction vessel bottom. The reaction vessel bottom is temperature controlled to $\pm 0.0005^{\circ}\text{C}$ and serves as a constant temperature heat sink. A controlled heater compensates for the energy liberated or absorbed by the reaction and the heat conducted to the reaction vessel bottom and maintains the isothermal cylinder at a constant temperature. The differences in the rates of energy supplied by the heater before, during, and after the reaction are a direct measure of the energy of the reaction. The frequency of electrical pulses ($0\text{--}10^5\text{ pulse s}^{-1}$) supplied to the heater is recorded on

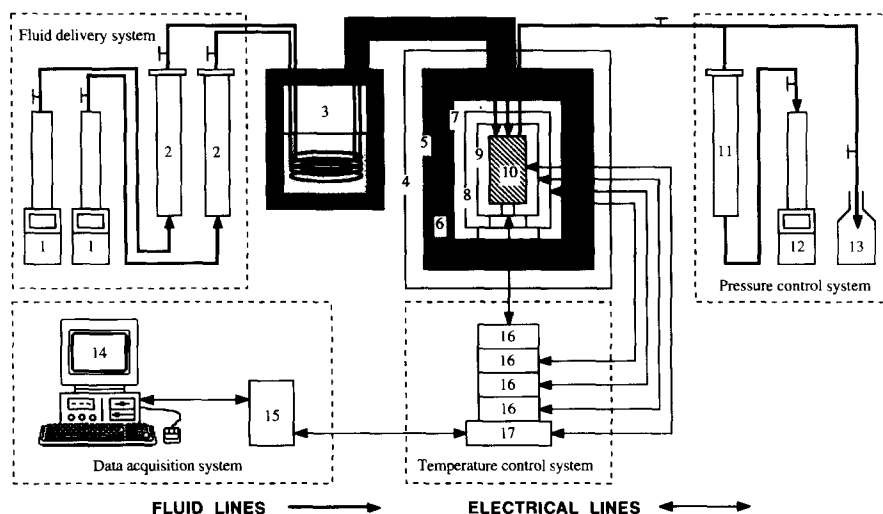


Fig. 1. Schematic diagram of the main components of the calorimeter: 1, pumps for fluid delivery; 2, pushers; 3, salt bath; 4, outer can; 5, insulating container; 6, fiberglass insulation; 7, outer shield; 8, inner shield; 9, reaction vessel; 10, isothermal cylinder; 11, waste solution reservoir; 12, pump for pressure control; 13, waste solution receiving bottle; 14, IBM-compatible computer; 15, computer interface; 16, Tronac PTC-41 temperature controllers; 17, Hart Scientific 3704 isothermal control unit.

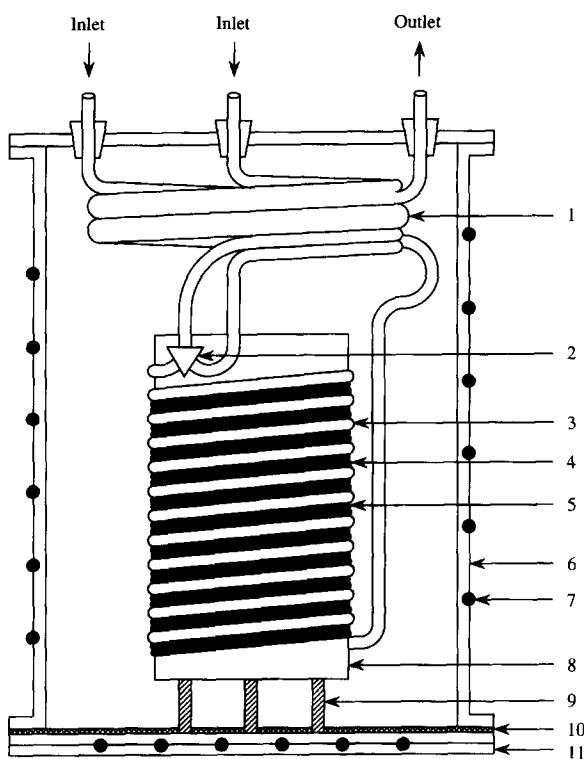


Fig. 2. Reaction vessel and contents: 1, heat exchanger; 2, mixing chamber; 3, equilibration coil; 4, calibration heater; 5, control heater; 6, reaction vessel wall; 7, heater; 8 isothermal cylinder; 9, heat-leak path; 10, asbestos insulation; 11, sandwich-type bottom plate.

the computer. Energy effects due to heats of mixing can be measured in the range $0.0025\text{--}2\text{ J s}^{-1}$ with a precision of $\pm 1.5\%$ or $\pm 0.0005\text{ J s}^{-1}$, whichever is greater.

2.1. Reaction vessel and isothermal cylinder

The nickel reaction vessel (9.5 cm ID, 12.7 cm high) contains the isothermal cylinder and the equilibration coil (Fig. 2). The nickel cylinder is 4.4 cm OD, 8.2 cm high, with a wall thickness of 0.238 cm at the top and 0.476 cm at the bottom. The bottom of the cylinder is closed and is 0.635 cm thick. The cylinder has three adjacent spiral grooves machined into its side, each having 15 turns. The grooves accommodate the equilibration coil tubing and Omegaclad wires used as the calibration heater and the control heater.

The equilibration coil is constructed of approximately 1.8 m of 1.588 mm OD, 0.396 mm wall thickness, platinum–10% rhodium tubing (Engelhard Corp., Iselin, NJ). The platinum–rhodium tubing was available in 1.22 m lengths. In order to obtain continuous tubing, the 1.22 m pieces were connected by gold brazing using 0.794 mm

OD, 0.198 mm wall thickness platinum–10% rhodium tubing as an inner sleeve. The sleeve length was about 1.5 cm for each union. All flow tubing used in the calorimeter was made of platinum–rhodium alloy and the total length is about 19.5 m.

Three thermistors (Thermometrics, Inc., Edison, NJ) with resistances of 1.0, 1.5, and 2.0 M Ω , respectively, at 125°C are attached with CC high-temperature cement (Omega Engineering, Inc., Stamford, CT) in the holes drilled near the bottom of the isothermal cylinder (Fig. 3). The thermistors are used to monitor continuously and control the cylinder temperature at a constant value. Three thermistors are used to cover the wide range of operating temperatures. Two 100 Ω (at 0°C) platinum resistance thermometers (PRT) (Omega Engineering, Inc., Stamford, CT) were also attached into holes drilled in the bottom of the isothermal cylinder and they are used to measure the absolute temperature of the cylinder. The PRTs were calibrated from 25 to 462°C using a Hart Scientific (Pleasant Grove, UT) 1006 digital thermometer which is traceable to IPTS-68. The absolute temperature can be measured to an accuracy of $\pm 0.1^\circ\text{C}$. The calibration and control heaters each consist of approximately 1.8 m of Omegaclad wire

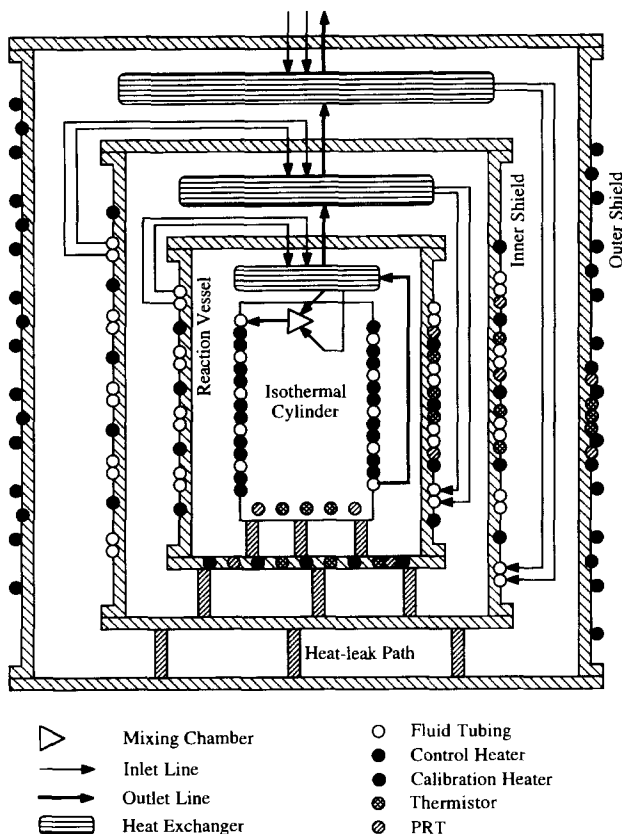


Fig. 3. Schematic of reaction vessel and thermal shields showing configuration of flow lines, heaters and temperature sensors.

No. 304-K-MO-040 (0.106 cm OD) (Omega Engineering, Inc., Stamford, CT) having a resistance of approximately $90\ \Omega$ (at 25°C), coiled in the spiral grooves cut in the side of the isothermal cylinder. The control heater and the appropriate thermistor, depending on the temperature range to be investigated, are connected to the Hart Scientific 3704 isothermal control unit. The temperature of the isothermal cylinder is controlled to $\pm 0.0005^\circ\text{C}$ (as indicated by the attached thermistors).

A heater comprised of a 0.5 m length of Omegaclad wire No. 304-K-MO-062 (0.159 cm OD) and having a resistance of approximately $11\ \Omega$ is coiled in a spiral groove in the sandwich-type bottom plate of the reaction vessel. Three thermistors (1.0, 1.5, and 2.0 $\text{M}\Omega$ at 125°C) are attached in the bottom plate with Omega CC high-temperature cement. The heater and a thermistor are connected to a Tronac (Orem, UT) PTC-41 temperature controller. The bottom plate of the reaction vessel is controlled to $\pm 0.0005^\circ\text{C}$ at a lower temperature than the isothermal cylinder. Three nickel bolts (0.635 cm OD, 1.27 cm in length) connect the bottom of the cylinder to the bottom of the reaction vessel. The spaces between the isothermal cylinder and the reaction vessel are filled with fiberglass insulation. The controlled temperature difference between the isothermal cylinder and the reaction vessel bottom serves as the driving force for heat conduction along the controlled heat-leak path (nickel bolts).

After entering the reaction vessel and before entering the equilibration coil, the reactants are equilibrated with the products from the coil in a countercurrent heat exchanger. This exchanger consists of 0.3 m lengths of the inlet and exit tubing which are wrapped together with silver wires, so that the two inlet streams run countercurrent to the exit stream. The two tubes containing the reactants are brought together in a triangular-shaped mixing chamber (made of platinum–10% iridium) as shown in Fig. 2. The two inlet tubes and the exit tube from the mixing chamber were connected to the mixing chamber by gold brazing.

Three thermistors (1.0, 1.5, and 2.0 $\text{M}\Omega$ at 125°C) are attached on the outside surface of the reaction vessel with Omega CC high-temperature cement. A 1.2 m length of Omegaclad wire No. 304-K-MO-062 having a resistance of approximately $27\ \Omega$ is coiled to the grooves cut on the outside surface of the reaction vessel. The heater and a thermistor are connected to a Tronac PTC-41 temperature controller. The side of the reaction vessel is controlled to $\pm 0.001^\circ\text{C}$ at the same temperature as the isothermal cylinder. The side and the bottom of the reaction vessel are insulated from each other by an asbestos blanket.

2.2. Thermal shields and insulating container

The inner and outer thermal shields consist of two nickel cans surrounding the reaction vessel as shown in Fig. 3. The inner shield has a 1.8 m length of Omegaclad wire No. 304-K-MO-062 with a resistance of about $39\ \Omega$ coiled into the grooves on its outside surface. Three thermistors (1.0, 1.5, and 2.0 $\text{M}\Omega$ at 125°C) are attached to the outside surface of the inner shield with Omega CC high-temperature cement. The heater and a thermistor are connected to a Tronac PTC-41 temperature controller and the temperature is controlled to $\pm 0.005^\circ\text{C}$. Two heaters are attached to the side of the outer shield. One heater consists of a 5.5 m length of Omegaclad wire No. 304-K-MO-

125 (0.318 cm OD) having a resistance of about 23Ω and is coiled in the grooves on the outside surface of the outer shield. The other heater consists of a 12.3 m length of Nichrome 60 wire No. 600 (0.083 cm OD) with ceramic insulation (Pelican Wire Company, Inc., Naples, FL) having a resistance of about 27Ω and is wrapped on the outside surface of the outer shield. Three thermistors (1.0, 1.5, and $2.0 \text{ M}\Omega$ at 125°C) are attached to the outside surface of the outer shield with Omega CC high-temperature cement. The heaters and a thermistor are connected to a Tronac PTC-41 temperature controller and the temperature is controlled to $\pm 0.01^\circ\text{C}$. A thermal path is provided from the reaction vessel to the shields through three 0.635 cm OD nickel bolts connecting the reaction vessel to the inner shield and the inner shield to the outer shield. The bolt circles are rotated at 60° between the two shields.

Two 100Ω (at 0°C) platinum resistance thermometers (PRT) are also attached with Omega CC high-temperature cement to the reaction vessel bottom and the outside surfaces of the reaction vessel and the thermal shields. The PRTs are used to monitor the temperatures of these various surfaces and to aid in setting their temperatures. All internal wiring in the calorimeter is 30 gauge, stranded, nickel-plated copper wire with glass wrap insulation. The upper operating temperature for this type of wire is approximately 500°C . Electrical connections inside the calorimeter are made by soldering with a silver-based alloy (BAg-1) containing copper, zinc, and cadmium. This type of material is subject to apparent oxidation by oxygen at temperatures above 350°C . The soldered connections are covered with Omega CC high-temperature cement and a small flow of argon gas is used to purge the calorimeter of air to minimize the oxidation.

The insulating container consists of a 38 cm OD stainless-steel can containing an 8 cm layer of Fiberfax S-Durablanket fiberglass insulation (Carborundum, Resistant Materials Co., Chicago, IL). The insulating container is surrounded by a 46 cm OD aluminum outer can which provides a 4 cm air gap between the outer can and the insulating container and has a small fan at its base to circulate air through the air gap.

2.3. Fluid delivery and pressure control

Two Isco (Lincoln, NE) 260D syringe pumps and two high-pressure pushers were used for the delivery of solutions to the calorimeter (Fig. 1). Each pump has a capacity of 266 ml with operational pressure from 0.1 to 51.7 MPa and flow rate from 0 to 2400 ml h^{-1} . Each of the pumps is equipped with a programmable controller. The controller has a liquid crystal display and the input is made through softkeys. Flow rate, pressure, and other operational parameters can be displayed on the controller front panel. The flow rates of the pumps were calibrated gravimetrically using distilled water and the accuracy was found to be better than $\pm 0.5\%$. The pump pressures were calibrated by 3D Instruments Inc. (Huntington Beach, CA) and the accuracy was $\pm 0.5\%$. The pumps are operated under the constant flow mode for fluid delivery and any flow ratio between the fluids can be introduced into the equilibration coil.

In order to prevent corrosion of the pumps by the electrolyte solutions, specially designed pushers were used. Solutions under study are contained in Teflon bags inside the pushers (Fig. 4). Pressure to transfer solutions to the calorimeter is transmitted by

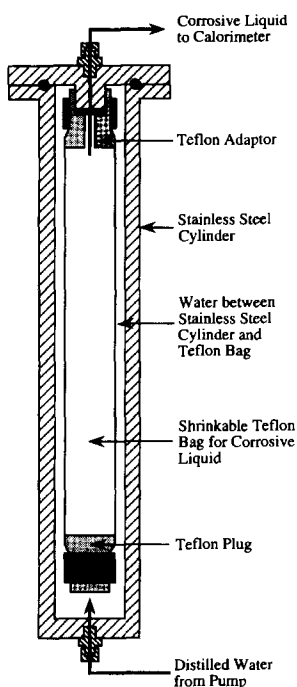


Fig. 4. Schematic of pusher.

water from the pumps to the pushers. The pushers were made of stainless-steel (7.8 cm OD, 5.2 cm ID, and 109.5 cm in length) with openings on the top cap and at the bottom. Each pusher has an adaptor machined from solid Teflon and attached to the top cap which supports a shrinkable Teflon bag (4.0 cm OD and 98.0 cm high). The Teflon bag was heat shrunk on the adaptor. The lower end of each Teflon bag is heat shrunk around a plug machined from solid Teflon.

In our previous flow calorimeters, the system pressure was controlled by a back pressure regulator. The control gas to the back pressure regulator was provided by a compressed nitrogen gas cylinder. The available pressure in the nitrogen gas cylinder limited the operational pressure of the calorimeter to 20 MPa. Use of the gas pressure control system at higher pressures presented a safety concern, as the highly compressed gas contains a large amount of energy. For operation of the calorimeter at higher pressures, we added an all-liquid pressure control system which consists of a new waste solution container and a pump running under the constant pressure mode. The waste solution container is exactly the same as the pushers used for fluid delivery. When the pump is operated under the constant pressure mode, the pressure is kept constant and the flow rate is automatically adjusted. The pressure stability attained with the all-liquid pressure control system is ± 0.01 MPa, which is better than the pressure stability of ± 0.07 MPa for our previous calorimeter [5], where nitrogen gas and a back pressure regulator were used for pressure control. The short-term noise in the

calorimetric signal is the same (± 100 pulse s^{-1}) for both the previous [5] and the present calorimeters.

2.4. Preheating and thermal equilibration

In order to achieve an isothermal condition in the isothermal cylinder, the inlet solutions must be brought to the temperature of the cylinder before they pass through the mixing chamber. We found that achieving an isothermal condition was difficult with previous calorimeters for operation above 325°C. This difficulty is understandable when we consider that there is a temperature difference of more than 300°C between the isothermal cylinder and the solutions in the Teflon bags. When the solutions entering the reaction zone are at lower temperatures than the cylinder temperature, there was a relatively large difference between the heats needed to maintain the cylinder at an isothermal condition with no solution flowing through the mixing chamber and with one solution flowing through. There must be enough preheating and thermal equilibration for the inlet solutions to attain the same temperature as the isothermal cylinder. To solve this problem, we used a salt bath (Fig. 1) in the present calorimeter.

The salt bath was made of a stainless-steel can (20.3 cm OD, 19.1 cm ID, and 22.9 cm high) with openings in the top plate for a stirrer, a thermocouple probe, and the tubing. The stainless-steel can was wrapped with fiberglass insulation. A salt mixture of sodium nitrate, sodium nitrite, and potassium nitrate was put in the salt bath and heated to the molten state. Control heaters were attached to the side and bottom of the salt bath. The heaters and a chromel–alumel thermocouple were connected to an Omega CN76000 controller. The salt bath is controlled at a temperature 50–100°C lower than the isothermal cylinder with a precision of $\pm 0.1^\circ\text{C}$. Before entering the calorimeter, the inlet solutions are preheated by passing through a 1.8 m length of platinum–rhodium tubing submerged in the salt bath. The portion of tubing between the salt bath and the calorimeter was wrapped with fiberglass insulation. Each of the inlet solutions was then thermally equilibrated to the temperature of the isothermal cylinder by passing through (1) a 1.2 m long countercurrent heat exchanger between the tops of the outer and inner shields, (2) a 1.8 m length of tubing wrapped on the outside surface of the inner shield, (3) a 0.8 m long countercurrent heat exchanger between the tops of the inner shield and the reaction vessel, (4) a 1.2 m length of tubing wrapped on the outside surface of the reaction vessel, and (5) a 0.3 m long countercurrent heat exchanger contained in the reaction vessel.

3. Procedure

All the temperature controllers are adjusted so that the calorimeter is operating at the desired temperature. The isothermal cylinder and the reaction vessel wall are set at the same temperature. The reaction vessel bottom is controlled at a temperature 0.5–1.5°C below the temperature of the isothermal cylinder. The inner shield is controlled at a temperature approximately 3°C lower than the temperature of the reaction vessel bottom. The outer shield is controlled at a temperature approximately

6°C lower than the inner shield temperature. A temperature gradient is thus provided for the heat generated in the equilibration coil to be transferred to the surrounding cans and room by conduction. The reaction vessel side wall temperature is finely adjusted by monitoring the heat pulse rate with no fluid and with one stream of fluid flowing through the coil. When the heat pulse rates are identical for both conditions, the temperature of the fluid entering the equilibration coil is assumed to be the same as the temperature of the isothermal cylinder. The exact temperature of the reaction vessel bottom is finely adjusted based on the amount of energy to be removed from the isothermal cylinder to balance the heat produced or absorbed by the reaction plus the heat provided by the isothermal control unit so that an appropriate heater pulse rate is achieved.

The pumps are filled with distilled water which is pumped into the pushers to expel the reactants into the calorimeter. A run consists, first, of running one pump at the total flow rate chosen for the reaction to determine a baseline heater pulse rate. Then, both pumps are run at their respective flow rates and the heater pulse rate determined for the reaction, followed by the other pump being run at the total flow rate and the baseline heater pulse rate being determined again. The calorimeter can be calibrated electrically by adding a known amount of heat through the calibration heater and measuring the resultant change in the control heater pulse rate. The precision for the electrical calibration constant (the energy equivalent of one pulse) is better than $\pm 0.5\%$.

4. Performance

Chemical calibrations were made on earlier versions of our flow calorimeters using the systems $\text{HClO}_4(\text{aq}) + \text{NaOH}(\text{aq})$ at 25°C [1], $\text{HClO}_4(\text{aq}) + \text{tris}(\text{hydroxymethyl})\text{aminomethane}(\text{aq})$ at 25°C [1], *n*-hexane + cyclohexane at 25°C [1,2], $\text{NaCl}(\text{aq}) + \text{water}$ at 50, 75, 100, and 125°C [7], ethanol + water at 75°C [7], 100°C [4], 110°C [2], and 140°C [2,3], hexane + toluene at 140°C [4], $\text{NaOH}(\text{aq}) + \text{water}$ at 250°C [5,6], and $\text{HCl}(\text{aq}) + \text{water}$ at 275°C [6]. Here (aq) represents aqueous solution. The calibrations showed that these calorimeters were capable of producing good calorimetric data over a wide range of temperature, pressure, flow rate, and concentration conditions. To test the performance of the present calorimeter, we determined the heats of dilution of 0.5148 M $\text{NaOH}(\text{aq})$ at 300°C (9.3 MPa) and of 0.5000 M $\text{NaCl}(\text{aq})$ at 300°C (9.3 MPa) and 350°C (17.6 MPa). Each of the measurements was repeated 3–5 times and the precision is often better than $\pm 1.5\%$.

The heats of dilution of 0.5148 M $\text{NaOH}(\text{aq})$ are compared in Table 1 with the results for 0.5146 M $\text{NaOH}(\text{aq})$ obtained using our previous flow calorimeter [12]. Since the uncertainty in the concentration of the NaOH solutions is about $\pm 0.2\%$, these two solutions can be considered as identical. It can be seen from the values in Table 1 that the agreement for $\text{NaOH}(\text{aq})$ is excellent.

Our results for the dilution of 0.5000 M $\text{NaCl}(\text{aq})$ are listed in Table 2 with some ΔH_{dil} values calculated using various information in the literature [23–25]. Busey et al. [23] measured heats of dilution of $\text{NaCl}(\text{aq})$ at selected conditions from 60 to 402°C and from 6.6 to 41.5 MPa. They presented equations for the apparent relative molar

Table 1
Heats of dilution (ΔH_{dil}) of 0.5148 M and 0.5146 M NaOH (aq) at 300°C, 9.3 MPa

This study			Literature ^c		
$m_i^a/$ (mol kg ⁻¹)	$m_f^b/$ (mol kg ⁻¹)	$\Delta H_{\text{dil}}/$ (kJ mol ⁻¹)	$m_i/$ (mol kg ⁻¹)	$m_f/$ (mol kg ⁻¹)	$\Delta H_{\text{dil}}/$ (kJ mol ⁻¹)
0.5148	0.4890	-0.714 ± 0.012	0.5146	0.4888	-0.708
0.5148	0.4634	-1.46 ± 0.02	0.5146	0.4632	-1.46
0.5148	0.4120	-3.09 ± 0.05	0.5146	0.4118	-3.08
0.5148	0.3606	-4.63 ± 0.06	0.5146	0.3605	-4.68
0.5148	0.3092	-6.56 ± 0.09	0.5146	0.3091	-6.57
0.5148	0.2577	-8.75 ± 0.13	0.5146	0.2576	-8.83
0.5148	0.2063	-11.52 ± 0.12	0.5146	0.2062	-11.47
0.5148	0.1548	-14.21 ± 0.21	0.5146	0.1547	-14.29
0.5148	0.1032	-18.43 ± 0.17	0.5146	0.1032	-18.30
0.5148	0.0516	-23.98 ± 0.26	0.5146	0.0516	-23.86
0.5148	0.0258	-28.17 ± 0.34	0.5146	0.0258	-27.79

^a Initial molality.

^b Final molality.

^c Ref. [12].

Table 2
Heats of dilution (ΔH_{dil}) of 0.5000 M NaCl(aq) at 300°C, 9.3 MPa and 350°C, 17.6 MPa

$m_i/$ (mol kg ⁻¹)	$\Delta H_{\text{dil}}/(\text{kJ mol}^{-1})$			
	This study	Busey et al. ^a	Archer ^b	Pitzer et al. ^c
		300°C, 9.3 MPa		
0.4496	-1.19 ± 0.03	-1.13	-1.24	-1.26
0.3993	-2.44 ± 0.04	-2.38	-2.60	-2.61
0.3490	-3.85 ± 0.04	-3.73	-4.11	-4.10
0.2989	-5.42 ± 0.06	-5.21	-5.81	-5.74
0.2489	-7.21 ± 0.08	-6.90	-7.75	-7.59
0.1989	-9.36 ± 0.13	-8.87	-10.01	-9.71
0.1490	-12.08 ± 0.12	-11.24	-12.75	-12.23
0.0993	-15.64 ± 0.18	-14.16	-16.23	-15.39
0.0496	-20.41 ± 0.23		-21.18	-19.84
		350°C, 17.6 MPa		
0.4496	-2.98 ± 0.05	-3.0		
0.3993	-7.04 ± 0.08	-6.7		
0.3490	-10.95 ± 0.14	-10.7		
0.2989	-15.78 ± 0.12	-14.9		
0.2488	-21.11 ± 0.28	-19.4		
0.1989	-27.81 ± 0.25	-24.8		
0.1490	-36.03 ± 0.44	-31.9		
0.0993	-46.36 ± 0.57	-41.6		

^a Calculated from the L_ϕ (apparent relative molar enthalpy) values in Table 5 and the pressure coefficients for L_ϕ in Table 7 of Ref. [23].

^b Calculated using the modified Pitzer ion-interaction model of Archer in Ref. [24].

^c Calculated using the Pitzer ion-interaction model of Pitzer et al. in Ref. [25].

enthalpy (L_ϕ) of NaCl(aq) based on the Pitzer ion-interaction model. They fitted the equations to their calorimetric data and reported values of fitting parameters. They also tabulated L_ϕ values for NaCl(aq) at round temperatures and the saturation pressure of water (Table 5 of Ref. [23]) and pressure coefficients of L_ϕ at round temperatures (Table 7 of Ref. [23]) from 100 to 350°C. We have attempted to reproduce their L_ϕ values at 300 and 350°C (at the saturation pressure) using their equations, fitting parameters, and pressure coefficients. But our calculation resulted in different L_ϕ values from those given by Busey et al. [23]. We do not have an explanation for this discrepancy. For comparison of our calorimetric data with those of Busey et al. [23], we calculated ΔH_{dil} values valid at our experimental condition from the tabulated values of L_ϕ and the pressure coefficients for L_ϕ in Ref. [23]. We can see from Table 2 that our ΔH_{dil} values are generally more negative than those calculated from the information given in Ref. [23], with the differences ranging from 1 to 10%.

Also given in Table 2 are ΔH_{dil} values at 300°C calculated from the models of Archer [24] and Pitzer et al. [25] for thermodynamic properties of NaCl(aq). Both Archer [24] and Pitzer et al. [25] used the calorimetric data of Busey et al. [23] up to 300°C, among various types of experimental data from other sources, in fitting their equations and obtaining fitting parameters. The model of Archer [24] extends to 325°C, while the model of Pitzer et al. [25] is valid only to 300°C. We can see from Table 2 that our ΔH_{dil} values are generally less negative than those calculated from these two models. At the present time, there are no satisfactory standard reference data for chemical calibration of high-temperature solution calorimeters. Nevertheless, we may still conclude from the results presented here that the calorimeter can produce good calorimetric data at high temperatures.

Acknowledgements

We express our appreciation to the National Science Foundation (Grant No. CHE-9223190) and the Army Research Office for financial support of this work.

References

- [1] J.J. Christensen, L.D. Hansen, D.J. Eatough, R.M. Izatt and R.M. Hart, *Rev. Sci. Instrum.*, 47 (1976) 730.
- [2] J.J. Christensen, L.D. Hansen, R.M. Izatt, D.J. Eatough and R.M. Hart, *Rev. Sci. Instrum.*, 52 (1981) 1226.
- [3] J.J. Christensen and R.M. Izatt, *Thermochim. Acta*, 73 (1984) 117.
- [4] J.J. Christensen, P.R. Brown and R.M. Izatt, *Thermochim. Acta*, 99 (1986) 159.
- [5] J.L. Oscarson, X. Chen, S.E. Gillespie and R.M. Izatt, *Thermochim. Acta*, 185 (1991) 51.
- [6] R.M. Izatt, J.L. Oscarson, S.E. Gillespie and X. Chen, *Determination of Thermodynamic Data for Modelling Corrosion*, EPRI Report NP-5708, Vol. 4, Electric Power Research Institute, Palo Alto, CA, 1992.
- [7] S.E. Gillespie, J.L. Oscarson, R.M. Izatt and P. Wang, *Thermochim. Acta*, 225 (1995) 71.
- [8] J.L. Oscarson, R.M. Izatt, P.R. Brown, Z. Pawlak, S.E. Gillespie and J.J. Christensen, *J. Solution Chem.*, 17 (1988) 841.

- [9] J.L. Oscarson, S.E. Gillespie, J.J. Christensen, R.M. Izatt and P.R. Brown, *J. Solution Chem.*, 17 (1988) 865.
- [10] S.E. Gillespie, J.L. Oscarson, X. Chen, R.M. Izatt and C. Pando, *J. Solution Chem.*, 21 (1992) 761.
- [11] J.L. Oscarson, S.E. Gillespie, R.M. Izatt, X. Chen and C. Pando, *J. Solution Chem.*, 21 (1992) 789.
- [12] X. Chen, S.E. Gillespie, J.L. Oscarson and R.M. Izatt, *J. Solution Chem.*, 21 (1992) 803.
- [13] X. Chen, S.E. Gillespie, J.L. Oscarson and R.M. Izatt, *J. Solution Chem.*, 21 (1992) 825.
- [14] X. Chen, J.L. Oscarson, S.E. Gillespie, H. Cao and R.M. Izatt, *J. Solution Chem.*, 23 (1994) 747.
- [15] J.L. Christensen, D.R. Cordray, J.L. Oscarson and R.M. Izatt, *J. Chem. Thermodyn.*, 20 (1988) 867.
- [16] P.W. Faux, J.J. Christensen and R.M. Izatt, *J. Chem. Thermodyn.*, 19 (1987) 1087.
- [17] J.J. Christensen, P.W. Faux, D.R. Cordray and R.M. Izatt, *J. Chem. Thermodyn.*, 18 (1986) 1053.
- [18] D.R. Cordray, J.J. Christensen, R.M. Izatt and J.L. Oscarson, *J. Chem. Thermodyn.*, 20 (1988) 877.
- [19] D.R. Cordray, J.J. Christensen and R.M. Izatt, *J. Chem. Thermodyn.*, 18 (1986) 581.
- [20] J.J. Christensen, D.M. Zebolsky and R.M. Izatt, *J. Chem. Thermodyn.*, 17 (1985) 183.
- [21] C. Pando, J.A.R. Renuncio, R.W. Hanks and J.J. Christensen, *Thermochim. Acta*, 63 (1983) 173.
- [22] D.R. Cordray, J.J. Christensen and R.M. Izatt, *Sep. Sci. Technol.*, 22 (1987) 1169.
- [23] R.H. Busey, H.F. Holmes and R.E. Mesmer, *J. Chem. Thermodyn.*, 16 (1984) 343.
- [24] D.G. Archer, *J. Phys. Chem. Ref. Data*, 21 (1993) 793.
- [25] K.S. Pitzer, J.C. Peiper and R.H. Busey, *J. Phys. Chem. Ref. Data*, 13 (1984) 1.